A particle representation model for the deformation of homogeneous turbulence

By S. C. Kassinos AND W. C. Reynolds

1. Motivation and objectives

In simple flows, where the mean deformation rates are mild and the turbulence has time to come to equilibrium with the mean flow, the Reynolds stresses are determined by the applied strain *rate*. Hence in these flows, it is often adequate to use an eddy-viscosity representation. The modern family of k-ϵ models has been very useful in predicting near equilibrium turbulent flows, where the rms deformation rate S is small compared to the reciprocal time scale of the turbulence (ϵ/k).

In modern engineering applications, turbulence models are quite often required to predict flows with very rapid deformations (large Sk/ϵ). In these flows, the structure takes some time to respond and eddy viscosity models are inadequate. The response of turbulence to rapid deformations is given by rapid distortion theory (RDT). Under RDT the nonlinear effects due to turbulence-turbulence interactions are neglected in the governing equations, but even when linearized in this fashion, the governing equations are unclosed at the one-point level due to the non-locality of the pressure fluctuations.

A good turbulence model should have a viscoelastic character, predicting turbulence stresses proportional to the mean strain rate (k-ϵ theory) for slow deformations and stresses determined by the amount of strain (RDT) for rapid deformations. Our goal has been the development of an engineering one-point model of turbulence that has this character. Our belief is that the greater modeling challenge is found in matching RDT when RDT applies. Hence our initial efforts were directed in constructing a good one-point model for RDT (Kassinos and Reynolds 1994).† Given a successful RDT model, we believe its blending with k-ϵ theory should be relatively straightforward. The success of the extended particle representation model (PRM) that will be discussed shortly provides justification for this point of view.

In a particle representation method, a number of key properties and their evolution equations are assigned to hypothetical particles. The idea is to follow an ensemble of "particles", determine the statistics of the ensemble, and use those as the representation for the one-point statistics of the corresponding field.

The key innovation in the original PRM approach presented in KR lies in the recognition that the linearity of the RDT governing equations makes it possible to emulate exactly the RDT for homogeneous turbulence using a PRM *without any modeling assumptions*. The non-local pressure effects can be evaluated within the framework of the PRM itself with no modeling assumptions. The PRM can be used

† Hereafter denoted by KR.

to evaluate all the one-point tensors needed in turbulence modeling, including the new structure tensors (see KR), but unlike spectral methods provides no two-point information. However, the PRM does provide information about the directional dependence of the real part of the spectrum of homogeneous turbulence. In that sense this method provides closure of RDT at minimum additional expense relative to a one-point approach.

The PRM has been used as the basis for the development of a viscoelastic *one-point* structure-based model of turbulence. Initially, the PRM was restricted to rapid mean deformations because our goal was to use it in developing a one-point model for the RDT of homogeneous turbulence (see KR). The development of the rapid *one-point* structure-based model has been completed with success, and we have recently been working on the extensions of the model to weak deformation rates and inhomogeneous flows. Towards that goal, we have extended the particle representation model to account for the non-linear turbulence-turbulence interactions that are important when the mean deformation is slow. This preliminary report discusses this Interacting Particle Representation Method (IPRM). As will be shown, the IPRM provides surprisingly accurate predictions for the one-point statistics in homogeneous turbulence subjected to a wide range of mean deformations. The IPRM is a viscoelastic structure-based model that bridges successfully RDT with k-ϵ theory. The success of the IPRM provides support to the idea that it should be easy to make a good model of RDT match k-ϵ theory when appropriate, and offers guidance in improving the slow extensions to the *one-point* structure-based model.

2. Accomplishments

In Sections 2.1 and 2.2 we introduce the basic RDT equations and the key ideas behind the PRM for the exact emulation of RDT. Then in Section 2.3, we present the formulation of the model for the non-linear particle-particle interactions (IPRM). In Section 2.4 we evaluate the IPRM for a wide range of mean deformations applied to homogeneous turbulence.

2.1 The basic RDT equations

The discussion is restricted to inviscid RDT because for the large eddies that contribute the most to the Reynolds stresses viscous effects are usually negligible, but this restriction can be removed. For the inviscid RDT of homogeneous turbulence, the fluctuating continuity and momentum equations are given by,

$$\frac{\partial u_i'}{\partial x_i} = 0 \tag{1}$$

and

$$\frac{\partial u_i'}{\partial t} + U_j \frac{\partial u_i'}{\partial x_j} = -G_{ij} u_j' - \frac{1}{\rho} p'_{,i}. \tag{2}$$

Here standard tensor notation is employed (subscripts after commas denote differentiation), U_i is the mean velocity, $G_{ij} = U_{i,j}$ is the mean velocity gradient tensor, and p' is the rapid part of the pressure fluctuations

$$\frac{1}{\rho} p'_{,mm} = -2G_{mn}u'_{n,m} \,. \tag{3}$$

We introduce the turbulent stream function vector defined by

$$u'_i = \epsilon_{its}\Psi'_{s,t} \qquad \Psi'_{i,i} = 0 \qquad \Psi'_{i,nn} = -\omega'_i \,. \tag{4}$$

We require Ψ'_i to be divergence-free so that the last equality in (4) is valid. This choice is important for the physical meaning of the resulting structure tensors introduced by Kassinos and Reynolds (see KR). Here ω'_i denotes the components of the turbulent vorticity vector. Note that Ψ'_i satisfies a Poisson equation and hence like the fluctuation pressure carries non-local information.

2.1.1 One-point structure tensors

The Reynolds stress tensor and the associated non-dimensional and anisotropy tensors are defined by

$$R_{ij} = \overline{u'_i u'_j} = \epsilon_{ipq}\epsilon_{jts}\overline{\Psi'_{q,p}\Psi'_{s,t}} \,, \qquad r_{ij} = R_{ij}/q^2 \,, \qquad \tilde{r}_{ij} = r_{ij} - \tfrac{1}{3}\delta_{ij} \,. \tag{5}$$

Here $q^2 = 2k = R_{kk}$. Introducing the isotropic tensor identity (Mahoney 1985)

$$\epsilon_{ipq}\epsilon_{jts} = \delta_{ij}\delta_{pt}\delta_{qs} + \delta_{it}\delta_{ps}\delta_{qj} + \delta_{is}\delta_{pj}\delta_{qt} - \delta_{ij}\delta_{ps}\delta_{qt} - \delta_{it}\delta_{pj}\delta_{qs} - \delta_{is}\delta_{pt}\delta_{qj} \tag{6}$$

and assuming homogeneity, one finds

$$R_{ij} + \underbrace{\overline{\Psi'_{k,i}\Psi'_{k,j}}}_{D_{ij}} + \underbrace{\overline{\Psi'_{i,k}\Psi'_{j,k}}}_{F_{ij}} = \delta_{ij}q^2 \,. \tag{7}$$

The constitutive Eq. (7) shows that for a proper characterization of non-equilibrium turbulence the *componentality* information found in r_{ij} must be supplemented by *structure* information found in the one-point turbulent *structure* tensors D_{ij} and F_{ij} introduced by KR [see Eq. (7)]. In addition to the basic definitions of these tensors that appear in (7), one can use equivalent representations for homogeneous turbulence in terms of the velocity spectrum tensor $E_{ij}(\mathbf{k})$ and vorticity spectrum tensor $W_{ij}(\mathbf{k})$. These are as follows:

• Structure *dimensionality* tensor

$$D_{ij} = \int \frac{k_i k_j}{k^2} E_{nn}(\mathbf{k}) \; d^3\mathbf{k} \qquad d_{ij} = D_{ij}/q^2 \qquad \tilde{d}_{ij} = d_{ij} - \tfrac{1}{3}\delta_{ij} \tag{8}$$

• Structure *circulicity* tensor

$$F_{ij} = \int \mathcal{F}_{ij}(\mathbf{k}) \; d^3\mathbf{k} \qquad f_{ij} = F_{ij}/q^2 \qquad \tilde{f}_{ij} = f_{ij} - \tfrac{1}{3}\delta_{ij} \,. \tag{9}$$

Here $\mathcal{F}_{ij}(\mathbf{k}) = k^2\overline{\hat{\Psi}_i\hat{\Psi}_j^*}$ is the circulicity spectrum tensor, which is related to the vorticity spectrum tensor $W_{ij}(\mathbf{k}) = \overline{\hat{\omega}_i\hat{\omega}_j^*}$ through the relation

$$\mathcal{F}_{ij}(\mathbf{k}) = \frac{W_{ij}(\mathbf{k})}{k^2}.$$

The familiar rapid pressure–strain-rate term is given by

$$T_{ij} = 2G_{ts}(M_{istj} + M_{jsti}) \tag{10}$$

where the fourth-rank tensor $\mathbf{M}$ is given by

$$M_{ijpq} = \int \frac{k_p k_q}{k^2} E_{ij}(\mathbf{k})\; d^3\mathbf{k}\,. \tag{11}$$

2.2 A particle representation of the RDT of homogeneous turbulence

The key innovation in the PRM approach of Kassinos and Reynolds (see KR) lies in the recognition that the linearity of the RDT governing equations makes it possible to emulate exactly the RDT for homogeneous turbulence using a PRM *without any modeling assumptions*. The non-local pressure effects can be evaluated within the framework of the PRM thus providing closure. This is unlike traditional particle representation approaches employed by the combustion community. In these traditional particle representations, usually in the form of PDFs, modeling assumptions are introduced at some level, usually to account for the effects of the fluctuating pressure gradient and molecular viscosity on the evolution of the particle velocity. One can take moments of the governing stochastic evolution equations to form equations for one-point statistics, like the Reynolds stresses. To each assumed stochastic model corresponds an equivalent one-point Reynolds Stress Transport (RST) model. Hence, it was common to assume a stochastic model that would produce one of the standard RST models, but in this way modeling was introduced where it was not needed, i.e. in matching RDT.

Next, we present the basic ideas behind the PRM for the emulation the RDT of homogeneous turbulence. A more detailed discussion of the rapid PRM can be found in KR.

2.2.1 Particle properties

We start with a discussion of the properties assigned to each of the hypothetical particles and a geometrical interpretation of the "particles". The assigned properties are:

- $\mathbf{V}$ velocity vector
- $\mathbf{W}$ vorticity vector
- $\mathbf{S}$ stream function vector
- $\mathbf{N}$ gradient vector
- P pressure.

These hypothetical particles represent an idealized building block for the turbulence structure. As shown in Fig. 1a, each particle corresponds to a plane of

independence. The vector **N**, which is normal to the plane of independence, provides a measure of gradients normal to the plane. The remaining vectors lie in the plane of independence. Thus, each particle represents a 1D-1C flow, similar to a vortex-sheet.

2.2.2 Vector identities between properties

We now turn to the vector identities that relate the basic properties assigned to each particle. These identities are motivated by the relationships that exist between the various vectors in a field of turbulence. In fact as it is next shown, a one-to-one correspondence exists between the field and PRM identities.

The three vectors **V**, **N**, and **W** form an orthogonal triad. The stream function vector **S** is related to **W** through the algebraic equation

$$S_i = -\frac{1}{N^2} W_i, \tag{12}$$

which is motivated by the Poisson Eq. (4). As a result of (12), we will often consider the vectors **V**, **N**, and **S** as the basic orthogonal vector triad (see Fig. 1a).

In a turbulence field, the fluctuation velocity is the curl of the fluctuation stream function [see (4)]; therefore the vector **V** is related to **S** and **N** through the analogous algebraic equation

$$V_i = \epsilon_{ipq} S_q N_p. \tag{13}$$

Equation (13) is a manifestation of the mutual orthogonality of the three vectors and can be used to show that

$$V^2 = S^2 N^2 \qquad V_i V_j + S_i S_j N^2 + N_i N_j S^2 = S^2 N^2 \delta_{ij}, \tag{14}$$

where $N^2 = N_i N_i$, $V^2 = V_i V_i$, and $S^2 = S_i S_i$. Note that (14) is the PRM analog of the constitutive Eq. (7).

The corresponding property unit vectors are denoted by lower case letters, that is

$$n_i = \frac{N_i}{N} \quad v_i = \frac{V_i}{V} \quad s_i = \frac{S_i}{S}. \tag{15}$$

Using (15), the constitutive Eq. (14) can be put into the form

$$v_i v_j + s_i s_j + n_i n_j = \delta_{ij}. \tag{16}$$

This is a direct consequence of the orthogonality of the three unit vectors **v**, **s**, and **n**. Equation (16) forms the basis for a number of identities relating higher products of property components.

2.2.3 Property evolution equations

We now turn to the evolution equations for the properties of each particle. The evolutions of **W** and **N** are governed by ordinary differential equations. The evolutions of **V** and **S** are determined through the algebraic Eqs. (12) and (13) that relate **V** and **S** to **W** and **N**.

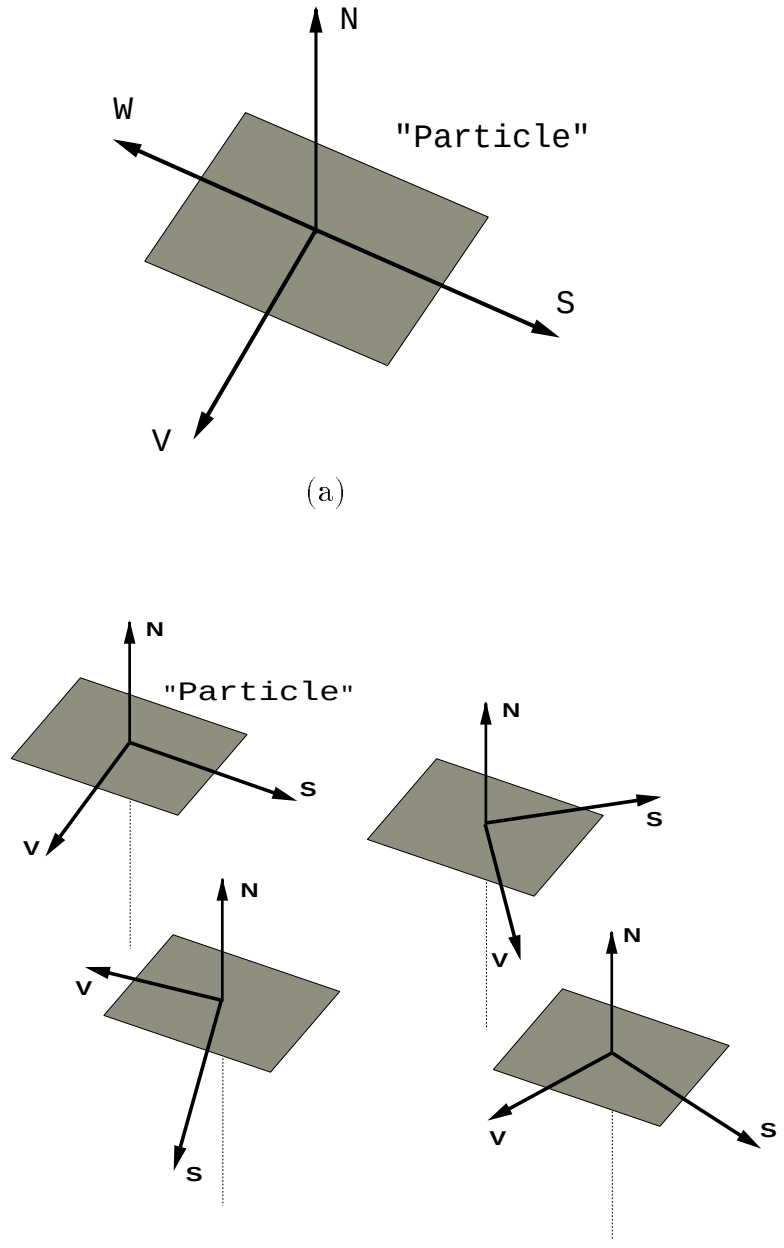

FIGURE 1. Particles used in the PRM: (a) The geometry associated with a hypothetical particle. (b) A cluster of particles forming 1D-2C flow.

A kinematic analysis of the motion of a plane of independence (vortex sheet) in a uniform mean deformation field (see KR) leads to the RDT evolution equation for $\mathbf{N}$

$$\dot{N}_i = -G_{ki} N_k. \tag{17}$$

The RDT equation for **W** is based on the exact RDT equation for the evolution of the fluctuating vorticity in homogeneous turbulence, and is

$$\dot{W}_i = G_{ik}W_k + \Omega_k V_i N_k - G_{kk}W_i. \tag{18}$$

The vector **S** is related to **W** through (12), which is analogous to the Poisson Eq. (4) connecting the turbulent vector stream function Ψ_i' to the fluctuation vorticity w_i'. Using the definition (12) and the evolution equations (17) and (18), one can derive the evolution equation for **S**

$$\dot{S}_i = G_{ik}S_k - \frac{\Omega_k V_i N_k}{N^2} - G_{kk}S_i + 2S_i G_{zk}\frac{N_z N_k}{N^2}. \tag{19}$$

As a consequence of (13), (17), and (19), one finds that the RDT evolution equation for **V** is

$$\dot{V}_i = -G_{ik}V_k + 2G_{km}\frac{V_m N_k N_i}{N^2}. \tag{20}$$

The Poisson equation for the rapid pressure (3) is the basis for the analogous definition

$$P = -2G_{km}\frac{V_m N_k}{N^2}, \tag{21}$$

which then allows (20) to be written as

$$\dot{V}_i = -G_{ik}V_k - PN_i \tag{22}$$

by analogy to the mean momentum equation. Note that the definition of a pressure in this context is optional and motivated by the desire to preserve the similarity of the basic PRM evolution equations to their field counterparts.

Equations analogous to the continuity equation and divergence-free vorticity condition,

$$V_i N_i = 0 \quad \text{and} \quad W_i N_i = 0 \tag{23}$$

are satisfied because **V** and **W** are perpendicular to **N**.

Note that one can evolve **V** and **N** with differential equations independently of any of the remaining variables and that the equations for the particle properties have a one-to-one correspondence with the comparable equations for the fields. The equivalence between the particle representation and the RDT field equations is discussed in detail in KR, where it is shown that **N** corresponds to the wavenumber vector **k**.

The evolution equations for the normalized gradient vector **n** will play an important role in the discussion that follows. This can be derived using the definition (15) along with (17) and is given by

$$\dot{n}_i = -G_{ki}n_k + G_{km}n_k n_m n_i\,. \tag{24}$$

2.2.4 Representation of one-point statistics

In this section we introduce the representation for the one-point statistics of the turbulence field in the context of the PRM. The Reynolds stress $R_{ij} = \overline{u_i' u_j'}$ is represented as

$$R_{ij} = \langle V_i V_j \rangle = \langle V^2 v_i v_j \rangle \,, \tag{25}$$

where the angle brackets denote averaging over an ensemble of particles. The structure-dimensionality $D_{ij} = \overline{\Psi'_{n,i} \Psi'_{n,j}}$ and structure circulicity $F_{ij} = \overline{\Psi'_{i,n} \Psi'_{j,n}}$ tensors are represented as

$$D_{ij} = \langle S_n S_n N_i N_j \rangle = \langle V^2 n_i n_j \rangle \qquad F_{ij} = \langle N_n N_n S_i S_j \rangle = \langle V^2 s_i s_j \rangle. \tag{26}$$

Similar representations exist for higher-rank tensors. For example, the representation for the fourth-rank tensor $\mathbf{M}$ [see (11)] appearing in the rapid pressure–strain-rate term is given by

$$M_{ijpq} = \langle V_i V_j n_p n_q \rangle = \langle V^2 v_i v_j n_p n_q \rangle. \tag{27}$$

2.2.5 PRM implementation: cluster-averaged method

Unless the evaluation of higher vector moments is required, the cluster-averaged implementation of the PRM described here should be preferred because it offers a better computational efficiency (see KR). The idea in the cluster-averaged method is to do the averaging in two steps, the first step being done analytically.

First, an averaging is done over particles that have the same $\mathbf{n}(t)$, followed by an averaging over all particles with different $\mathbf{n}(t)$. The one-point statistics resulting from the first (cluster) averaging are conditional moments, which will be denoted by

$$R_{ij}^{|\mathbf{n}} \equiv \langle V_i V_j | \mathbf{n} \rangle \qquad D_{ij}^{|\mathbf{n}} \equiv \langle V^2 n_i n_j | \mathbf{n} \rangle = \langle V^2 | \mathbf{n} \rangle n_i n_j \qquad F_{ij}^{|\mathbf{n}} \equiv \langle V^2 s_i s_j | \mathbf{n} \rangle. \tag{28}$$

The conditionally averaged stress evolution equation

$$\dot{R}_{ij}^{|\mathbf{n}} = -G_{ik} R_{kj}^{|\mathbf{n}} - G_{jk} R_{ki}^{|\mathbf{n}} + 2 G_{km} (R_{im}^{|\mathbf{n}} n_k n_j + R_{jm}^{|\mathbf{n}} n_k n_i) \tag{29}$$

is obtained by using the definition (28) along with (21) and (22). Note that (24) and (29) are *closed* for the conditional stress tensor $R_{ij}^{|\mathbf{n}}$ and n_i. That is, they can be solved without reference to the other conditioned moments. Thus, to follow the evolution of R_{ij}, instead of following a large number of particles that carry $\mathbf{V}$ and $\mathbf{n}$ with simple evolution equations (direct method), we can follow a smaller number of *particle clusters* that carry $\mathbf{R}^{|\mathbf{n}}$ and $\mathbf{n}$ with only slightly more complicated evolution equations. These particle clusters correspond to 1D-2C vortical flows (vortex sheets) as shown in Fig. 1b. The conditioned stresses must satisfy $R_{ip}^{|\mathbf{n}} n_p = 0$ and this property will be maintained by (24) and (29) if it is initially true. Note that it is unnecessary to evolve the conditioned $F_{ij}^{|\mathbf{n}}$ equation, since the constitutive Eq. (14) can be used to obtain $F_{ij}^{|\mathbf{n}}$ (and hence F_{ij}) from the evolved $R_{ij}^{|\mathbf{n}}$ and n_i.

Finally it is important to appreciate that the choice of $\mathbf{n}$ as the *cluster vector* to be evolved in the cluster-averaged method is important. Unlike the evolution equations for the $\langle\ |\mathbf{n}\rangle$ conditioned moments, the equations for the $\langle\ |\mathbf{s}\rangle$ and $\langle\ |\mathbf{v}\rangle$ moments are not closed and require modeling.

2.3. The interacting particle representation model (IPRM)

When the time scale of the mean deformation is large compared to that of the turbulence, the nonlinear turbulence-turbulence interactions become important in the governing field equations. In the context of the IPRM, these nonlinear processes are represented by particle-particle interactions. As in the case of the one-point field equations, the nonlinear processes cannot be evaluated directly and modeling is required. Because some modeling must be introduced, the emulation of the field equations by the IPRM is no longer exact, which was the case for the PRM emulation of RDT.

2.3.1 Formulation of the slow model

Here we present what we have termed the Interacting Particle Representation Method (IPRM). The basic idea behind the IPRM is simple. The overall effect of the background particle-particle interactions on any given particle is modeled in two parts. The first part, which we call the *effective gradient* model, assumes that the background particle-particle interactions provide a gradient acting on the particles in addition to the mean deformation rate. The assumption is that the effective deformation rate can be expressed in terms of the mean deformation rate and statistics based on the particle ensemble thus providing closure.

The second part of the particle-particle interaction model accounts for rotational effects. Mean rotation acting on the particles tends to produce rotational randomization of the $\mathbf{V}$ vectors around the $\mathbf{n}$ vectors (see KR). Effective rotation due to particle-particle interactions should also induce a similar randomization effect. We have found that best results are obtained when this *slow rotational randomization effect* is modeled explicitly.

Different models for the effective eddy deformation tensor are possible, and we are still exploring some of these options. Here we report one such model that we have found to produce excellent results for irrotational mean strain and good results for homogeneous shear, and the elliptic streamline flows (Blaisdell & Shariff 1994). We are using this IPRM as a guide in extending the structure-based model to flows with weak mean deformation.

Direct numerical simulations (see Kassinos & Reynolds 1995) show that under weak strain the structure dimensionality $\mathbf{D}$ remains considerably more isotropic than do the Reynolds stresses $\mathbf{R}$. Hence we modify the basic equations (17) and (22) for the evolution of the particle properties to account for these effects:

$$dN_i = - \underbrace{G^n_{ki} N_k \, dt}_{\text{effective gradient}} \tag{30}$$

$$dV_i = - \underbrace{G^v_{ik} V_k \, dt}_{\text{effective gradient}} + P N_i \, dt - \underbrace{C_1 \, V_i \, dt - C_2 \, V \epsilon_{ipq} d\mathcal{W}_p n_q}_{\text{slow rotational randomization}} . \tag{31}$$

The effective gradients are given by

$$G^n_{ij} = G_{ij} + \frac{C^n}{\tau} r_{ik} d_{kj} \qquad G^v_{ij} = G_{ij} + \frac{C^v}{\tau} r_{ik} d_{kj} \, . \tag{32}$$

Here $G_{ij} = U_{i,j}$ is the mean gradient tensor, and τ is the time scale of the turbulence, which as explained below is evaluated so that the dissipation rate $\epsilon^{\rm PRM}$ in the IPRM [Eq. (39)] matches that obtained from a standard model equation for ϵ. The constants C^v and C^n are taken to be $C^n = 2.2C^v = 2.2$. The different values for these two constants account for the different rates of return to isotropy of $\mathbf{D}$ and $\mathbf{R}$. However, note that the same tensor $r_{ik}d_{kj}$ accounts for the effective eddy deformation rate seen by both N_i and V_i.

The *slow rotational randomization* (SRR) model provides a random rotation of the $\mathbf{V}$ about the $\mathbf{n}$ vector such that the orthogonality of the two vectors is preserved. The "stochastic" character of this correction is introduced through the Wiener process $d\mathcal{W}_i(t)$ (see Kassinos and Reynolds 1995, Durbin and Speziale 1994). The increments of the Wiener process are steps of the random walk and provide Gaussian white-noise forcing (Arnold 1974). The properties of these increments are

$$\overline{d\mathcal{W}_i} = 0 \qquad \overline{d\mathcal{W}_i d\mathcal{W}_j} = dt\delta_{ij} \qquad \overline{V_j\, d\mathcal{W}_i} = 0\,. \tag{33}$$

The second property in (33) shows that the Wiener process has magnitude $d\mathcal{W} = O(dt)^{1/2}$; therefore $d\mathcal{W}_i/dt$ is not defined as $dt \to 0$. Hence, in order to evaluate $d(V_iV_j)/dt$, we first form the product

$$d(V_iV_j) = (V_i + dV_i)(V_j + dV_j) - V_iV_j\,. \tag{34}$$

One can use (31), (33), and (34) to form the cluster-averaged equations (see Section 2.2.5)

$$\dot{n}_i = -G^n_{ki}n_k + G^n_{kr}n_kn_rn_i \tag{35}$$

$$\begin{aligned}\dot{R}^{|\mathbf{n}}_{ij} &= -G^v_{ik}R^{|\mathbf{n}}_{kj} - G^v_{jk}R^{|\mathbf{n}}_{ki} \\ &\quad + [G^n_{km} + G^v_{km}](R^{|\mathbf{n}}_{im}n_kn_j + R^{|\mathbf{n}}_{jm}n_kn_i) \\ &\quad - [2C_1R^{|\mathbf{n}}_{ij} - C_2^2R^{|\mathbf{n}}_{kk}(\delta_{ij} - n_in_j)]\,.\end{aligned} \tag{36}$$

We require the that rotational randomization model leaves the conditional energy unmodified. This requires that $C_1 = C_2^2$, and hence using dimensional considerations we take

$$C_r = C_1 = C_2^2 = \frac{8.5}{\tau}\,\Omega^*\, f_{pq}n_pn_q \qquad \Omega^* = \sqrt{\Omega^*_k\Omega^*_k} \qquad \Omega^*_i = \epsilon_{ipq}r_{qk}d_{kp}\,. \tag{37}$$

Note that the rotational randomization coefficient C_r is sensitized to the orientation of the $\mathbf{n}$ vector so that the effective rotational randomization vanishes whenever the large-scale circulation is confined in the plane normal to $\mathbf{n}$. This effect is similar to the material indifference to mean rotation condition, which requires the rotational randomization to vanish whenever $\Omega_kn_k = 0$. By definition $C_r \geq 0$ and this property is satisfied by $f_{pq}n_pn_q > 0$ because f_{ij} is positive definite.

The pressure P is determined by the requirement that $V_k N_k = 0$ is maintained by (35) and (36). This determines the effects of the slow pressure strain−rate-term without the need for further modeling assumptions

$$P = \underbrace{2G_{mk}\frac{V_k N_m}{N^2}}_{\text{rapid}} + \underbrace{\frac{(C^v + C^n)}{\tau} r_{mt} d_{tk} \frac{V_k N_m}{N^2}}_{\text{slow}} . \tag{38}$$

The rate of dissipation of the turbulent kinetic energy $k = \frac{1}{2}q^2$ that is produced by the IPRM Eq. (36) is given by

$$\epsilon^{\text{PRM}} = q^2 \frac{C^v}{\tau} r_{ik} d_{km} r_{mi} . \tag{39}$$

To complete the IPRM we use the standard model equation for the dissipation rate (ϵ) with a rotational modification to account for the suppression of ϵ due to mean rotation,

$$\dot{\epsilon} = -C_0(\epsilon^2/q^2) - C_s S_{pq} r_{pq} \epsilon - C_\Omega \sqrt{\Omega_n \Omega_m d_{nm}}\, \epsilon . \tag{40}$$

Here Ω_i is the mean vorticity vector, and the constants are taken to be

$$C_0 = -\tfrac{11}{3} \qquad C_s = -3 \qquad \text{and} \qquad C_\Omega = 0.01 .$$

We choose the time scale τ so that $\epsilon^{\text{PRM}} = \epsilon$. This requires that

$$\tau = (\frac{q^2}{\epsilon}) C^v r_{ik} d_{km} r_{mi} . \tag{41}$$

2.4 Evaluation of the IPRM

In this section, the IPRM given by (35), (36), (40), and (41) is evaluated for five independent homogeneous flows. The evaluation of the IPRM for rapid mean deformation (large Sk/ϵ) is reported in detail in KR, where it is shown that given enough particles, the IPRM reproduces the *exact* RDT results. Therefore, in this section, we report only on the performance of the IPRM for flows involving weak mean deformation (small Sk/ϵ), where the nonlinear interactions are important.

2.4.1 Homogeneous shear in a rotating frame

We first consider the problem of homogeneous shear in a rotating frame. The mean velocity gradient tensor G_{ij}, the frame vorticity Ω_i^f, and frame rotation rate Ω_i are defined by

$$G_{ij} = \begin{pmatrix} 0 & S & 0 \\ 0 & 0 & 0 \\ 0 & 0 & 0 \end{pmatrix} , \qquad 2\Omega_i = \Omega_i^f = (0, 0, \Omega^f) . \tag{40}$$

We consider initially isotropic turbulence with

$$r_{ij} = \tfrac{1}{3}\delta_{ij}, \qquad k = k_0 , \qquad \epsilon = \epsilon_0 . \tag{41}$$

First, we consider the case of homogeneous shear in a stationary frame ($\Omega^f = 0$) with an initial $Sk_0/\epsilon_0 = 2.36$. The IPRM predictions for the components of the normalized Reynolds stress tensor r_{ij} are shown in Fig. 2. The symbols are from the direct numerical simulation (DNS) of Rogers and Moin (1986), which also had $Sk_0/\epsilon_0 = 2.36$. The agreement between the IPRM predictions and the DNS results is good, but the IPRM somewhat overpredicts r_{11} and underpredicts r_{22}. Figure 3 shows the evolution of the dimensionless parameters P/ϵ and Sk/ϵ. Again, the IPRM predictions (lines) are in good agreement with DNS results (symbols), especially in the period $8 \lesssim St \lesssim 15$ where the DNS was fully developed. The same equilibrium values are predicted for the two dimensionless parameters by both the DNS simulation and the IPRM. As shown in Table 1, the equilibrium state predicted by the model is also in reasonable agreement with the experiments of Tavoularis & Karnik (1989).

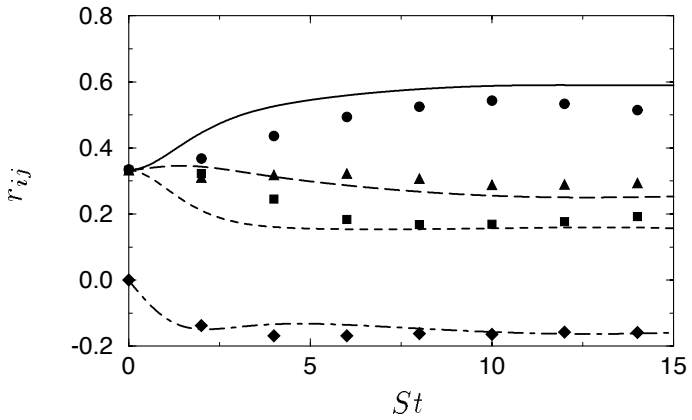

FIGURE 2. Time evolution of the normalized Reynolds stress tensor $r_{ij} = R_{ij}/R_{kk}$ in homogeneous shear flow ($Sk_0/\epsilon_0 = 2.36$). Comparison of the IPRM predictions (lines) with the direct numerical simulations (symbols) of Rogers and Moin (1986); 11 component (——— , •), 22 component (- - - - , ■), 33 component (— — — , ▲), 12 component (—·— , ♦).

The solution in the case of homogeneous shear in a rotating frame depends on the initial conditions only through the dimensionless parameter Sk_0/ϵ_0 and on the frame vorticity through the dimensionless parameter Ω^f/S (Speziale *et al.* 1991). The value of Ω^f/S determines whether the flow is stable in which case k and ϵ decay in time, or unstable in which case both k and ϵ grow exponentially in time.

The effect of the ratio Ω^f/S on the time evolution of the normalized kinetic energy k/k_0 is shown in Fig. 4. In the absence of DNS or experimental data, we evaluate the model performance using the large-eddy simulations of Bardina *et al.* (1983). Note that the model captures the general trends correctly. For example, it correctly predicts that the highest rate of growth (for both k and ϵ) occurs for $\Omega^f = S/2$, which RDT shows is the most unstable case. It also predicts a weak rate of decay for the case $\Omega^f = S$ and a decay (relaminarization) for $\Omega^f = -S$. The numerical agreement with the LES is reasonable, but the model tends to predict somewhat

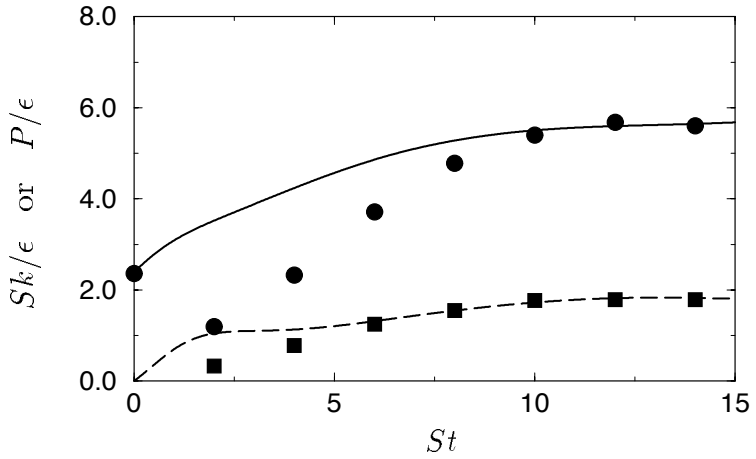

FIGURE 3. Time evolution of the nondimensional parameters Sk/ϵ (——— , •) and P/ϵ (– – – – , ■) in homogeneous shear flow. IPRM predictions (lines) are compared to the DNS (symbols) of Rogers and Moin (1986).

lower rates of growth, particularly so in the case $\Omega^f = 0.5S$. This problem is also common to all the currently available second-order closures as noted by Speziale *et al.* (1989). However, a detailed comparison of numerical values is probably not meaningful in this case because the reported LES results came from the filtered field only.

2.4.2 Irrotational axisymmetric strain

Next, we consider the performance of the IPRM for two cases of axisymmetric contraction and two cases of axisymmetric expansion. The mean velocity gradient tensor is given by

$$S_{ij} = \begin{pmatrix} S & 0 & 0 \\ 0 & -S/2 & 0 \\ 0 & 0 & -S/2 \end{pmatrix} \tag{42}$$

with $S > 0$ for contraction and $S < 0$ for expansion. We consider homogeneous turbulence with an initially isotropic state as specified in (41). The solution depends on the initial conditions through the non-dimensional parameter Sk_0/ϵ_0. Comparisons are made with the DNS of Lee & Reynolds (1985).

The dimensionless strain parameter

$$C^* = \exp\left(\int_0^t |S_{\max}(t')|\, dt' \right) \tag{43}$$

will serve as the time coordinate for the comparison of the IPRM to the DNS results.

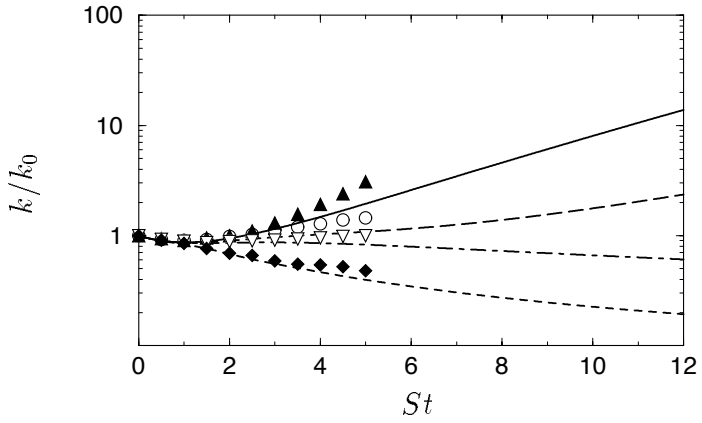

FIGURE 4. Time evolution of the turbulent kinetic energy in rotating shear flows. IPRM predictions (lines) are compared to the LES of Bardina *et al.* (symbols): $\Omega^f/S = 0$ (– – – – , ○), $\Omega^f/S = 0.5$ (——— , ▲), $\Omega^f/S = 1.0$ (—·— , ▽), and $\Omega^f/S = -1.0$ (– – – – , ◆).

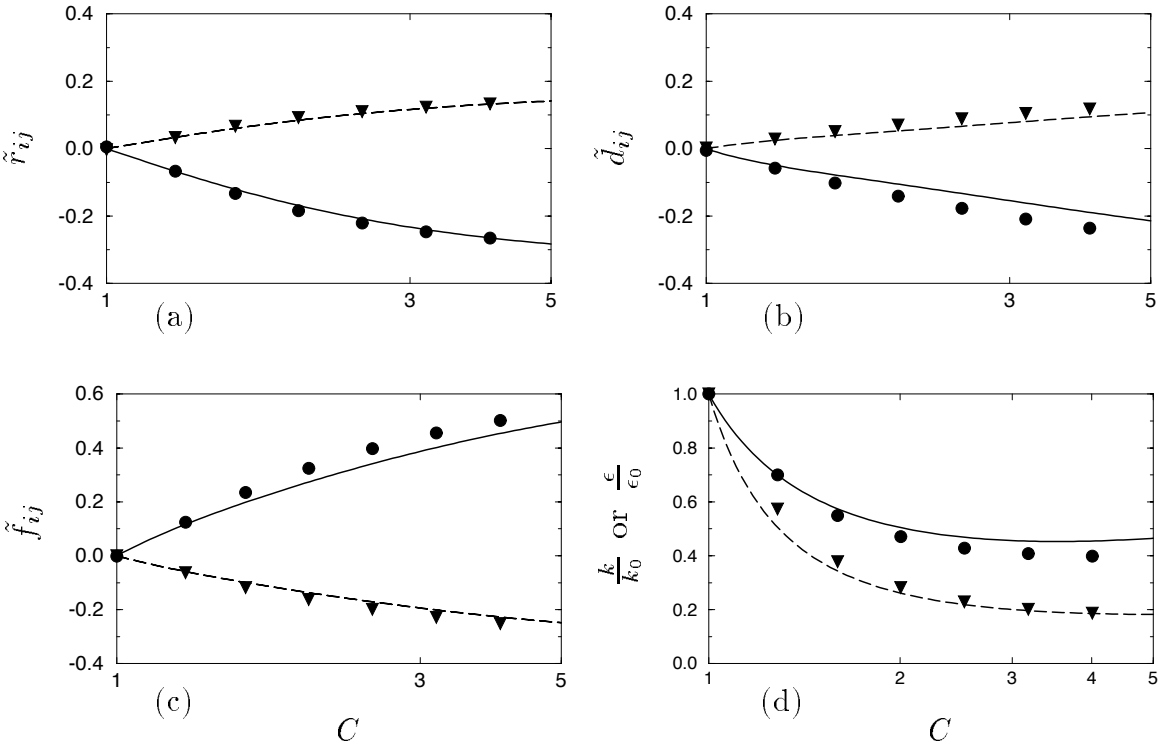

FIGURE 5. Comparison of IPRM predictions (shown as lines) with the DNS of Lee & Reynolds (1985) for axisymmetric contraction case AXK ($Sq_0^2/\epsilon_0 = 1.1$). Evolution of the (a) Reynolds stress, (b) dimensionality, and (c) circulicity anisotropies: 11 component (——— , •), 22 and 33 components (– – – – , ▼). (d) evolution of the normalized turbulent kinetic energy (——— , •) and dissipation rate (– – – – , ▼).

Equilibrium Values	IPRM	Experiments
r_{11}	0.59	0.51 ± 0.04
r_{22}	0.16	0.22 ± 0.02
r_{33}	0.25	0.27 ± 0.03
r_{12}	-0.16	-0.16 ± 0.01
Sk/ϵ	5.97	4.60 ± 0.50
P/ϵ	1.86	1.47 ± 0.14

TABLE 1. Equilibrium results for homogeneous shear: comparison with the experiments of Tavoularis & Karnik (1989).

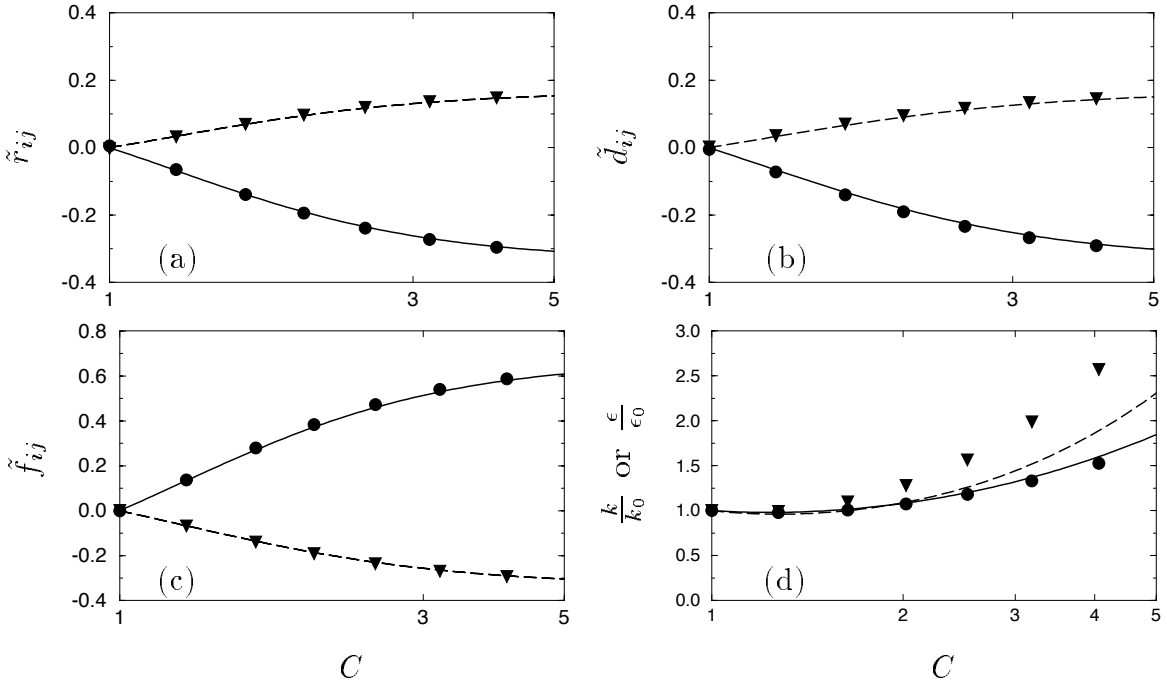

FIGURE 6. Comparison of IPRM predictions with the DNS of Lee & Reynolds (1985) for axisymmetric contraction case AXL ($Sq_0^2/\epsilon_0 = 11.1$). Evolution of (a) the Reynolds stress, (b) dimensionality, and (c) circulicity anisotropies. (d) Evolution of the normalized turbulent kinetic energy and dissipation rate. Symbols as in Fig. 5.

Axisymmetric contraction flow

The IPRM predictions for two cases of irrotational axisymmetric contraction are shown in Figs. 5 and 6. In both cases, the IPRM predictions (lines) for the evolution of the anisotropies $\tilde{\mathbf{r}}$, $\tilde{\mathbf{d}}$, and $\tilde{\mathbf{f}}$ are in good agreement with the DNS results (symbols). The IPRM predicts decay of the turbulent kinetic energy k and dissipation rate ϵ for the weaker strain case $[Sq_0^2/\epsilon_0 = 1.1]$ and growth in the more rapid run $[Sq_0^2/\epsilon_0 = 11.1]$. This is in agreement with the DNS results; however, the

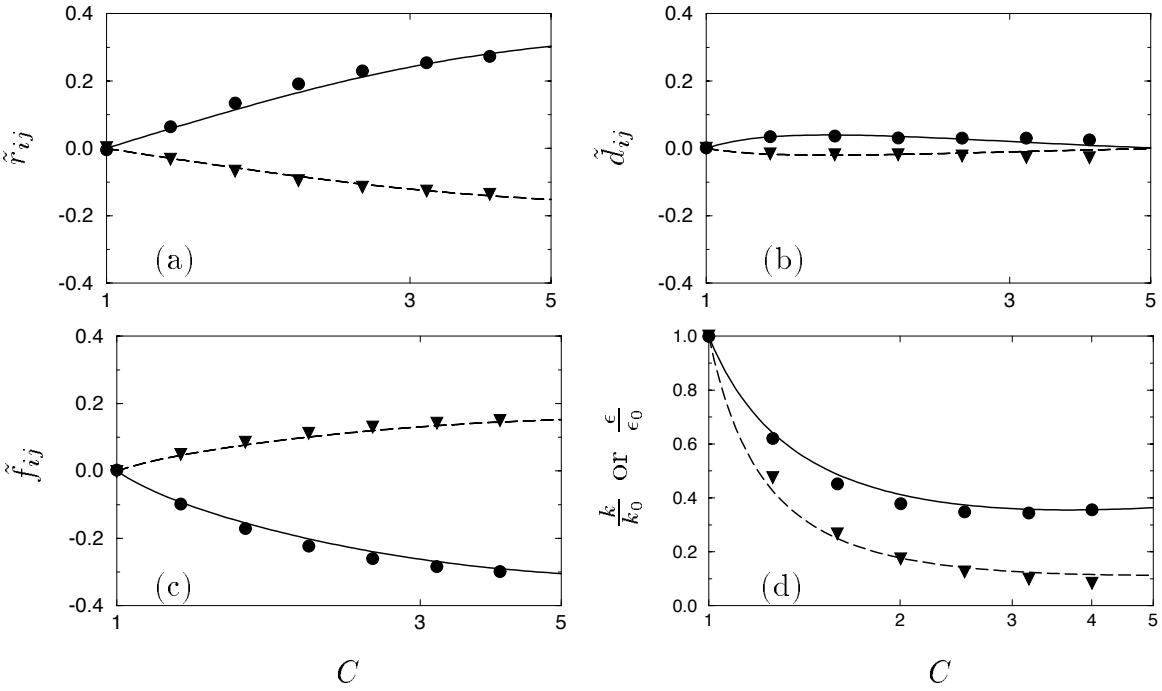

FIGURE 7. Comparison of IPRM predictions (shown as lines) with the DNS of Lee & Reynolds (1985) for axisymmetric expansion case EXO ($Sq_0^2/\epsilon_0 = 0.82$). Evolution of the (a) Reynolds stress, (b) dimensionality, and (c) circulicity anisotropies: 11 component (——— , •), 22 and 33 components (– – – – , ▼). (d) evolution of the normalized turbulent kinetic energy (——— , •) and dissipation rate (– – – – , ▼).

predicted rate of growth for ϵ in this second case is too weak as compared to the DNS result (see Fig. 6d). This difference is related to the model Eq. (40) used for the dissipation rate and not directly to the IPRM equations. We believe that we can improve on this aspect of the IPRM, but feel this refinement should follow once we have investigated various alternative models for the effective eddy deformation $r_{ik}d_{kj}$.

Axisymmetric expansion flow

The IPRM predictions for two cases of irrotational axisymmetric expansion are shown in Fig. 7 for $Sq_0^2/\epsilon_0 = 0.82$ and Fig. 8 for $Sq_0^2/\epsilon_0 = 8.2$. Comparison is again made with the DNS of Lee & Reynolds. As was discussed in Kassinos & Reynolds (1995), the axisymmetric expansion flows exhibit a paradoxical behavior where a weaker mean deformation rate produces a stress anisotropy that exceeds the one produced under RDT. This effect is triggered by the different rates of return to isotropy in $\mathbf{r}$ and $\mathbf{d}$ equations, but it is dynamically controlled by the rapid terms. The net effect is a growth of $\tilde{\mathbf{r}}$ in expense of $\tilde{\mathbf{d}}$, which is strongly suppressed.

As shown in Fig. 7, the IPRM is able to capture these intriguing effects quite accurately despite the relatively simple model used for the particle-particle interactions. This success of the IPRM points to the fact that these unexpected effects, once triggered, are driven by the rapid terms: the IPRM representation of the rapid

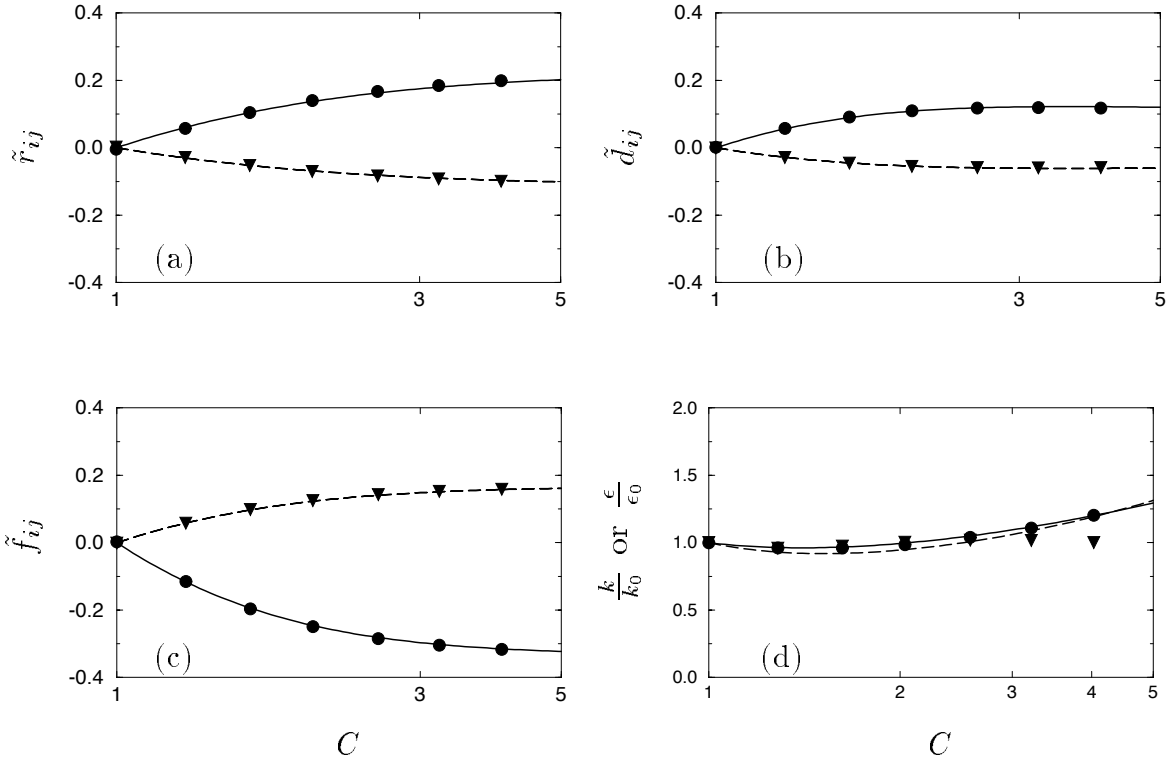

FIGURE 8. Comparison of IPRM predictions with the DNS of Lee & Reynolds (1985) for axisymmetric expansion case EXP ($Sq_0^2/\epsilon_0 = 8.2$). Evolution of (a) the Reynolds stress, (b) dimensionality, and (c) circulicity anisotropies. (d) Evolution of the normalized turbulent kinetic energy and dissipation rate. Symbols as in Fig. 7.

terms is exact and this enables it to capture these intriguing effects. The IPRM predictions for the evolution of the turbulent kinetic energy k and dissipation rate ϵ are also quite accurate.

Plane strain

The performance of the IPRM in the case of the irrotational plane strain flows is shown in Fig. 9 for $Sq_0^2/\epsilon_0 = 1.0$ and Fig. 10 for $Sq_0^2/\epsilon_0 = 8.0$. The DNS of Lee & Reynolds (1985) is used for the comparison. The IPRM predictions for the evolution of the anisotropies $\tilde{\mathbf{r}}$, $\tilde{\mathbf{d}}$, and $\tilde{\mathbf{f}}$ are in very good agreement with the DNS results. Note that the value of the initial Sq_0^2/ϵ_0 has a strong effect on the distribution of the $\tilde{d}_{ij}$ components and the IPRM is able to capture these effects quite well. The evolution histories for the normalized turbulent kinetic energy and dissipation rate are shown in Figs. 9d and 10d. The predictions are in good agreement with the DNS results, displaying decay for $Sq_0^2/\epsilon_0 = 1.0$ and growth for $Sq_0^2/\epsilon_0 = 8.0$ at the correct rates.

2.4.3 Elliptic streamline flow

The elliptic streamline flows combine the effects of mean rotation and plane strain and emulate the conditions encountered in the flow through various sections of turbomachinery. These relatively basic flows provide a challenging test case for

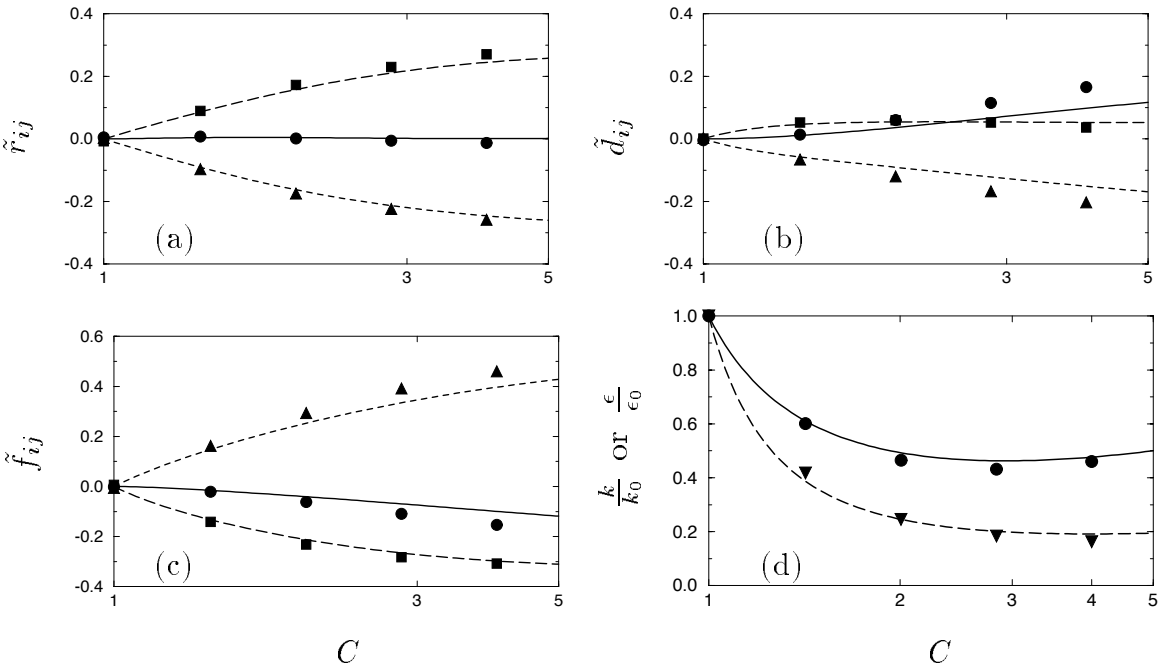

FIGURE 9. Comparison of IPRM predictions (shown as lines) with the DNS of Lee & Reynolds (1985) for plane strain case PXA ($Sq_0^2/\epsilon_0 = 1.0$). Evolution of the (a) Reynolds stress, (b) dimensionality, and (c) circulicity anisotropies: 11 component (——— , •), 22 component (– – – – , ■), and 33 component (– – – – , ▲). (d) evolution of the normalized turbulent kinetic energy (——— , •) and dissipation rate (– – – – , ▼).

turbulence models. For example, direct numerical simulations show exponential growth of the turbulent kinetic energy in elliptic streamline flows, but standard k-ϵ models (as well as most Reynolds stress models) predict decay of the turbulence. The structure-based model (Reynolds & Kassinos 1995) does predict an exponential growth, but not yet at the correct rate.

The elliptic streamline flow corresponds to a mean deformation tensor of the form

$$G_{ij} = \begin{pmatrix} 0 & 0 & -\gamma - e \\ 0 & 0 & 0 \\ \gamma - e & 0 & 0 \end{pmatrix}$$

with $0 < |e| < |\gamma|$. Note that the case $e = 0$ corresponds to pure rotation while the case $|e| = |\gamma|$ corresponds to homogeneous shear. The elliptic streamlines in this flow have an aspect ratio given by $E = \sqrt{(\gamma + e)/(\gamma - e)}$. As explained by Blaisdell and Shariff (1994), the important nondimensional parameters for the elliptic streamline flow are (1) the aspect ratio E of the elliptic streamlines and (2) the ratio of the turbulent time scale to the time scale of the mean deformation. The turbulent Reynolds number is also an important parameter, but the IPRM model is based on a high Reynolds number assumption. The IPRM predictions are shown in Fig. 11 for three different cases, which are summarized in Table 2.

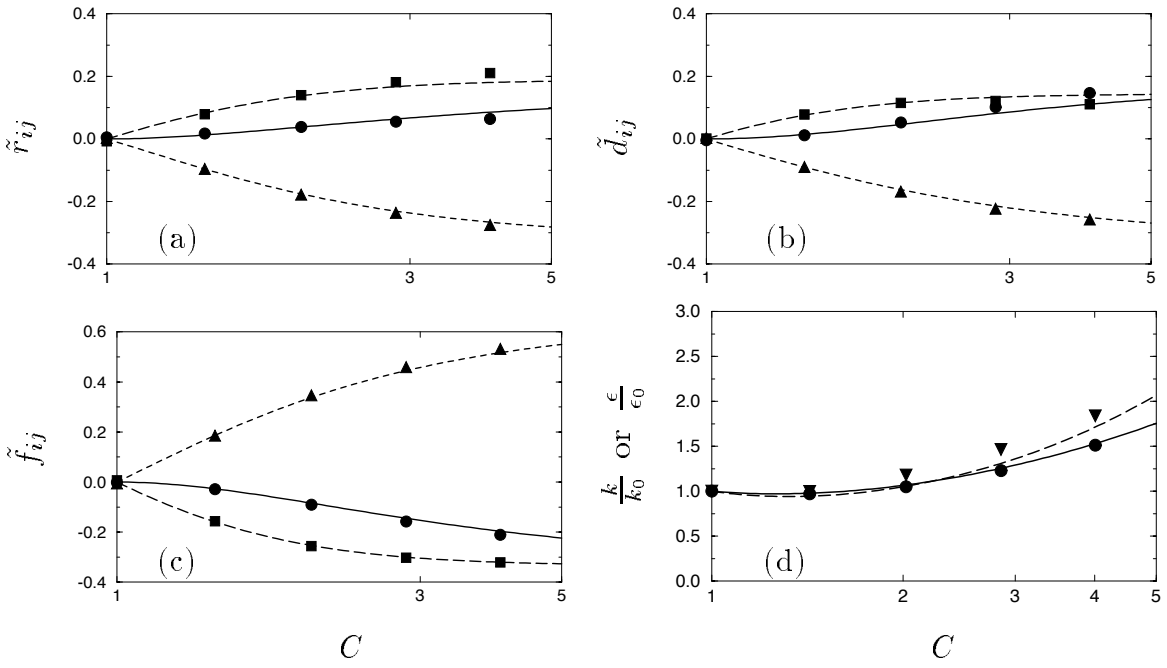

FIGURE 10. Comparison of IPRM predictions with the DNS of Lee & Reynolds (1985) for plane strain case PXD ($Sq_0^2/\epsilon_0 = 8.0$). Evolution of (a) the Reynolds stress, (b) dimensionality, and (c) circulicity anisotropies. (d) Evolution of the normalized turbulent kinetic energy and dissipation rate. Symbols as in Fig. 9.

The notation used here is identical to the one introduced by Blaisdell and Shariff (1994). For example, $S_e^* = \epsilon k/\epsilon$ represents the ratio of the turbulent time scale to the mean flow time scale based on the mean strain. We have evaluated the IPRM predictions using preliminary results from the simulations of Blaisdell and found its performance to be very good. The IPRM predicts exponential growth for the turbulent kinetic energy and dissipation rate at the correct rates of growth. The IRPM predictions for the individual components of the Reynolds stress anisotropy tensor were also in very good agreement with the corresponding DNS predictions from those preliminary runs. Here we only report the predictions of the IPRM, and postpone any comparison to DNS till final results are available from the simulations of Blaisdell.

Case	E	$S^*_{\epsilon_0}$
e3	1.5	1.68691
e4	2.0	1.68691
e2	1.25	1.68691

TABLE 2. Initial conditions for the elliptic streamline cases.

3. Summary and future plans

In simple flows with mild mean deformation rates the turbulence has time to

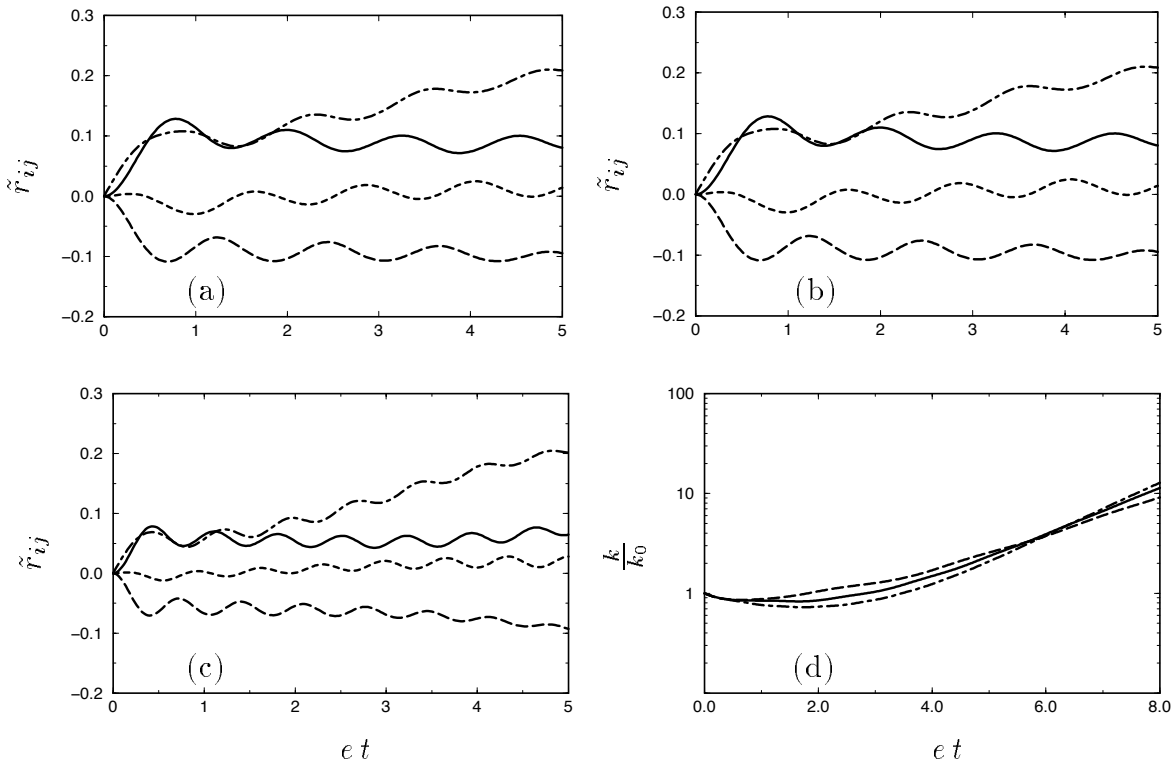

FIGURE 11. IPRM predictions for the evolution of the Reynolds stress anisotropy components in elliptic streamline flow with (a) E=1.5 , (b) E=2.0, and (c) E=1.25: 11 component, ——— ; 22 component, – – – – ; 33 component, – – – – ; 13 component, —·— . (d) Evolution of the normalized turbulent kinetic energy in elliptic streamline flow: E=1.5, ——— ; E=2.0, – – – – ; E=1.25, —·— .

come to equilibrium with mean flow and the Reynolds stresses are determined by the strain *rate*. On the other hand, when the mean deformation is very rapid, the turbulent structure takes some time to respond and the Reynolds stresses are determined by the amount of *total* strain.

A good turbulence model should exhibit this viscoelastic character of turbulence, matching the two limiting behaviors and providing a reasonable blend in between. Our goal has been the development of one-point model for engineering use with the proper viscoelastic character. We have shown that to achieve this goal one needs to include structure information in the tensorial base used in the model because non-equilibrium turbulence is inadequately characterized by the turbulent stresses themselves. We have also argued that the greater challenge in achieving viscoelasticity in a turbulence model is posed by the matching of rapid distortion theory (RDT). Given a good RDT model, we believe its extension to flows with mild deformation rates should be relatively straightforward.

The interacting particle representation model (IPRM) presented here provides strong support for this position. The IPRM is in essence a very good viscoelastic,

structure-based turbulence model. As it was shown here, with a relatively simple model for the nonlinear turbulence-turbulence interactions, the IPRM is able to handle quite successfully a surprising wide range of flows. Some of these flows involve paradoxical effects, and the fact that the IPRM is able to reproduce them suggests that perhaps the model captures a significant part of the underlying physics.

We believe that the success of the IPRM is based on its firm core, that is its exact representation of RDT. We have used the rapid version of the IRPM in constructing a one-point structure-based model for RDT, now completed successfully. We are currently using the IPRM in extending the one-point model to flows with mild deformation rates. We are also investigating further extensions to the IPRM that might enable it to become a valuable engineering tool on its own right.

REFERENCES

ARNOLD, L. 1974 *Stochastic Differential Equations.* John Wiley and Sons.

BARDINA, J., FERZIGER, J. H., & REYNOLDS, W. C. 1983 Improved turbulence models based on large eddy simulation of homogeneous, incompressible, turbulent flows. *Report TF-19,* Thermosciences Division, Department of Mechanical Engineering, Stanford University.

BLAISDELL, G. A. & SHARIFF, K. 1994 Homogeneous turbulence subjected to mean flow with elliptic streamlines. *Proceedings of the 1994 Summer Program.* Center for Turbulence Research, NASA Ames/Stanford Univ., 355-371.

DURBIN, P. A. & SPEZIALE, C. G. 1994 Realizability of second-moment closures via stochastic analysis. *J. Fluid Mech..* **280,** 395-407.

LEE, M. J. & REYNOLDS, W. C. 1985 Numerical experiments on the structure of homogeneous turbulence. *Report TF-24,*Thermosciences Division, Department of Mechanical Engineering, Stanford University.

MAHONEY, J. F. 1985 Tensor and Isotropic Tensor Identities. *The Matrix and Tensor Quarterly.* **34(5),** 85-91.

KASSINOS, S. C. AND REYNOLDS, W. C. 1994 A structure-based model for the rapid distortion of homogeneous turbulence. *Report TF-61,* Thermosciences Division, Department of Mechanical Engineering, Stanford University.

KASSINOS, S. C. AND REYNOLDS, W. C. 1995 An extended structure-based model based on a stochastic eddy-axis evolution equation. *Annual Research Briefs 1995*, Center for Turbulence Research, NASA Ames/Stanford Univ., 133-148.

ROGERS, M. M., MOIN, P. 1987 The structure of the vorticity field in homogeneous turbulent flows. *J. Fluid. Mech.* **176,** 33-66.

TAVOULARIS, S. & KARNIK, U. 1989 Further experiments on the evolution of turbulent stresses and scales in uniformly sheared turbulence. *J. Fluid. Mech.* **204,** 457-478.